

Central Lancashire Online Knowledge (CLoK)

Title	Marker based and markerless motion capture for equestrian rider kinematic
	analysis: A comparative study
Type	Article
URL	https://clok.uclan.ac.uk/id/eprint/55378/
DOI	https://doi.org/10.1016/j.jbiomech.2025.112728
Date	2025
Citation	Cameron-Whytock, Heather, Divall, Hannah, Lewis, Martin and Apps, Charlotte (2025) Marker based and markerless motion capture for equestrian rider kinematic analysis: A comparative study. Journal of Biomechanics, 186. p. 112728. ISSN 0021-9290
Creators	Cameron-Whytock, Heather, Divall, Hannah, Lewis, Martin and Apps, Charlotte

It is advisable to refer to the publisher's version if you intend to cite from the work. https://doi.org/10.1016/j.jbiomech.2025.112728

For information about Research at UCLan please go to http://www.uclan.ac.uk/research/

All outputs in CLoK are protected by Intellectual Property Rights law, including Copyright law. Copyright, IPR and Moral Rights for the works on this site are retained by the individual authors and/or other copyright owners. Terms and conditions for use of this material are defined in the http://clok.uclan.ac.uk/policies/

ELSEVIER

Contents lists available at ScienceDirect

Journal of Biomechanics

journal homepage: www.elsevier.com/locate/jbiomech



Marker based and markerless motion capture for equestrian rider kinematic analysis: A comparative study

Heather Cameron-Whytock a,b,* D, Hannah Divall c, Martin Lewis d, Charlotte Apps c

- ^a School of Veterinary Medicine, University of Central Lancashire, Preston PR1 2HE, UK
- ^b School of Animal Rural and Environmental Science, Nottingham Trent University, Brackenhurst Campus, Southwell NG25 OQF, UK
- ^c School of Science and Technology, Nottingham Trent University, Clifton Campus, Clifton NG11 8NS, UK
- ^d Qualisys Europe, Qualisys AB, Göteberg 411 05, Sweden

ARTICLEINFO

Keywords:
Equestrian
Rider
Kinematics
Deep Learning
Markerless Motion Capture

ABSTRACT

The study hypothesised that a markerless motion capture system can provide kinematic data comparable to a traditional marker-based system for riders mounted on a horse. The objective was to assess the markerless system's accuracy by directly comparing joint and segment angle measurements taken during walking and trotting with those obtained from a marker-based system. Ten healthy adult participants performed five dynamic trials during walking and trotting. A twelve-camera marker-based system and eight-camera 2D video-based system were synchronised. Three-dimensional hip, knee, shoulder and elbow joint angles, and the global trunk and pelvis angle were computed for comparison between the two systems. To assess the error between systems, the root mean square difference (RMSD) was averaged across each gait cycle and statistical parametric mapping (SPM) paired t-tests were applied. The sagittal trunk angle had the lowest RMSD of 2.0° and elbow rotation had the highest RMSD of 19°, with the same values for walking and trotting. SPM indicated increased hip flexion (0–100 %, p < 0.001) and elbow flexion (24–47 %, p = 0.03; 63–100 %, p < 0.001) in the walking gait cycle for the markerless system. A lack of joint range of motion and obscured medial limbs during walking whilst mounted on horses may cause increased offsets for markerless data in equestrian riders. No significant differences were found for the transverse plane, yet there tended to be increased RMSD. This lack of consistency suggests results from the transverse plane in equestrian riders should be interpreted with caution. Study findings indicate that markerless technology has the potential to be a suitable alternative to marker-based systems for assessment of equestrian riders, dependent on the segment/joint angle of interest and the level of acceptable error. These results indicate that markerless systems can effectively be utilised for rider biofeedback, though their application may be limited for specific joint analyses.

1. Introduction

Biomechanical analysis in equestrian sport is valuable for assessing the horse, rider, and both in combination. Previous research has used biomechanical analysis to assess kinematics and kinetics of riding racehorses (Walker et al., 2016), investigate differences in rider movement patterns (Byström et al., 2015), and quantify trunk kinematics of experienced versus novice riders (Clark et al., 2022). However, research in this field is limited, with few studies focusing on the rider.

Kinematic analysis of equestrian riders is typically conducted using marker-based motion capture systems, where retroreflective markers are affixed to key anatomical points (Byström et al., 2015; Engell et al.,

2016; Rhodin et al., 2018). Despite being the most common method, marker-based analysis has several practical limitations: (1) attaching markers is time-consuming, especially for full-body three dimensional (3D) analysis, (2) accurate marker placement can be affected by human error, (3) data quality may be compromised by marker displacement due to skin/clothing movement, (4) markers may detach during dynamic assessment, leading to missing anatomical points, and (5) data processing is skill-intensive and time-consuming. Additionally, marker-based kinematic analysis may restrict movement or be impractical in some settings such as competition (Strutzenberger et al., 2021).

Novel markerless techniques have been recently developed for assessing human locomotion, which overcome limitations of marker-

^{*} Corresponding author at: School of Veterinary Medicine, University of Central Lancashire, Preston PR1 2HE, UK.

E-mail addresses: hcameron-whytock@uclan.ac.uk (H. Cameron-Whytock), hannah.divall@ntu.ac.uk (H. Divall), martin.lewis@qualisys.com (M. Lewis), charlotte.apps@ntu.ac.uk (C. Apps).

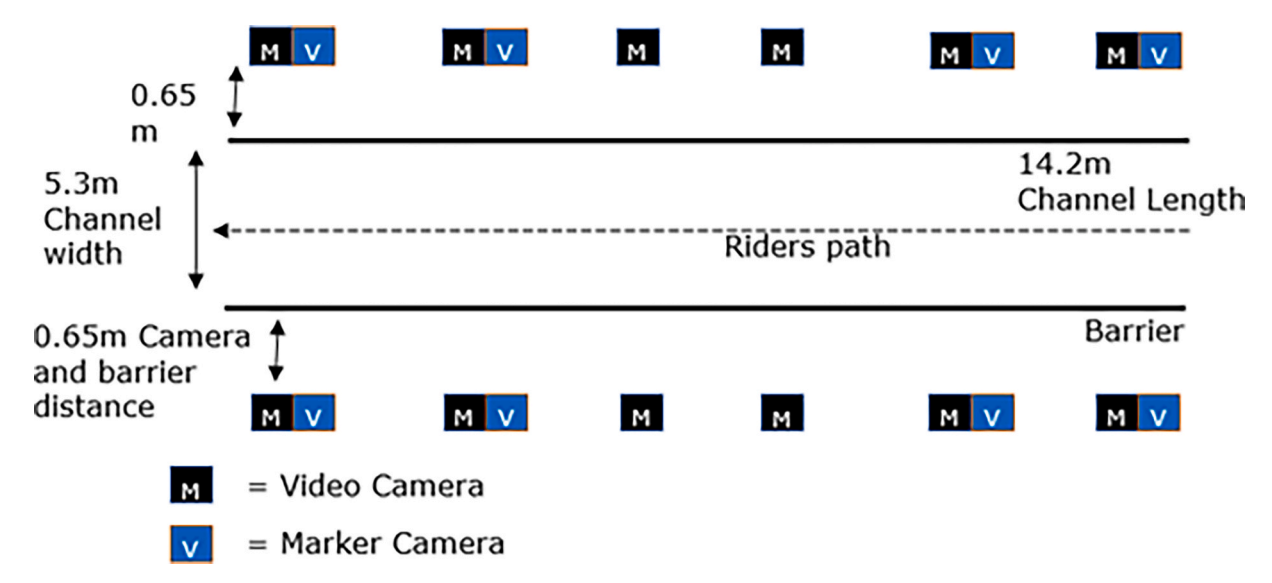


Fig. 1. Schematic of the testing layout.

Table 1Mean (SD) Root Mean Square Errors (°) in the sagittal, frontal and transverse planes for walking and trotting. Joint angle results are reported for the left and right sides.

		Sagittal		Frontal		Transverse	
		Walk	Trot	Walk	Trot	Walk	Trot
Elbow	Left	6.9	9.5			16.1	13.9
		(1.2)	(1.6)			(2.7)	(3.0)
	Right	6.0	8.1			19.1	18.8
		(1.2)	(1.2)			(3.9)	(4.1)
Shoulder	Left	4.55	4.3	5.58	7.2	8.0	10.9
		(1.3)	(1.2)	(1.1)	(1.2)	(1.6)	(2.5)
	Right	4.9	5.1	5.5	6.1	9.8	7.0
		(1.2)	(1.0)	(1.2)	(1.0)	(1.6)	(1.9)
Knee	Left	7.3	7.0	10.1	7.5	7.5	10.8
		(2.3)	(1.7)	(2.2)	(3.7)	(2.2)	(2.7)
	Right	7.3	6.1	10.4	9.1	9.4	10.5
		(1.0)	(1.6)	(1.8)	(1.7)	(2.4)	(2.5)
Hip	Left	12.3	8.5	5.6	5.3	8.7	8.7
		(1.8)	(2.4)	(1.1)	(1.1)	(2.0)	(2.3)
	Right	13.2	7.8	4.4	4.3	9.0	9.9
		(1.9)	(2.0)	(1.2)	(1.0)	(2.0)	(1.9)
Pelvis Segment		2.7	2.7	8.1	5.1	2.9	2.8
		(0.8)	(0.7)	(1.7)	(1.6)	(0.8)	(0.9)
Trunk Segment		2.0	2.0	4.9	5.2	2.9	2.0
		(0.5)	(0.6)	(1.3)	(0.8)	(1.5)	(0.6)
Mean		6.7	6.1	6.8	5.0	9.3	9.5
		(3.7)	(2.5)	(2.4)	(3.0)	(5.1)	(4.9)

based systems. These systems have been validated for jumping (Strutzenberger et al., 2021), functional activities (Song et al., 2023), and gait (Wren et al., 2023). This technology has the potential to improve kinematic analysis in equestrian sports and expand data collection opportunities in this field. For example, equestrian sports such as eventing expose participants to risk of injury and fatality, with 54 rider fatalities and 171 horse fatalities reported between 2000–2023 (Bennet et al., 2023b). A key risk factor for fatalities in eventing is horse falls during cross-country, where the horse hits a jumping obstacle at speed and falls, sometimes landing on top of and crushing the rider (Bennet et al., 2022).

Despite identifying horse falls as a key risk factor, research in eventing has largely been limited to retrospective studies (Bennet et al., 2022, 2023a; Cameron-Whytock et al., 2024) and estimation-based methods like computer simulations, which often fail to replicate real-life scenarios (Foreman et al., 2019). Collecting real-time kinematic

data during high-risk events like horse falls is challenging due to ethical and logistical constraints, such as the inability to capture data during competition and the impracticality of replicating such events in field settings. As a result, biomechanical research in equestrian sports remains limited, especially regarding real-time rider kinematics.

Traditional methods for investigating horse falls rely on retrospective data and computational modelling, as gathering real-time kinematic data on falls is challenging. Marker-based systems are intrusive in competition settings and could interfere with performance, while replicating falls for research is ethically unjustifiable due to the injury risks (Bennet et al., 2022).

Markerless motion capture systems offer a promising alternative. These systems enable non-intrusive data collection during live competition or training, eliminating the need for physical markers that may interfere with the rider. Markerless systems have the potential to advance biomechanical research in equestrian sports by overcoming the limitations of traditional methods and facilitating real-world studies of rider kinematics.

Markerless data could provide insights into how a rider's balance, posture and movement affect the dynamics of the horse during a fall and contribute to injuries. In addition, markerless technology could be utilised within rider-feedback systems for training and coaching, or for the purposes of therapy such as aiding return from physical injury. Alternative technologies like inertial measurement units (IMU) are not restricted by camera capture volumes (Gandy et al., 2014), but IMU measurements have limitations such as drift, magnetic interference, and difficulty calibrating body placement (Stanev et al., 2021). Poor concurrence in the transverse and frontal planes may be due to different algorithms used in IMU systems compared to marker-based models (Robert-Lachaine et al., 2017; Zhang et al., 2013).

The objective of this study was to evaluate the feasibility and accuracy of a markerless motion capture system for assessing equestrian rider kinematics during walking and trotting, compared to a marker-based system. We hypothesised that the markerless system would provide data comparable to the marker-based system.

2. Materials and methods

2.1. Ethical Research

The study was approved by Nottingham Trent University ethics committee, ID: 1546070, and conducted in compliance with UK and EU laws on animal research. Procedures adhered to the Declaration of

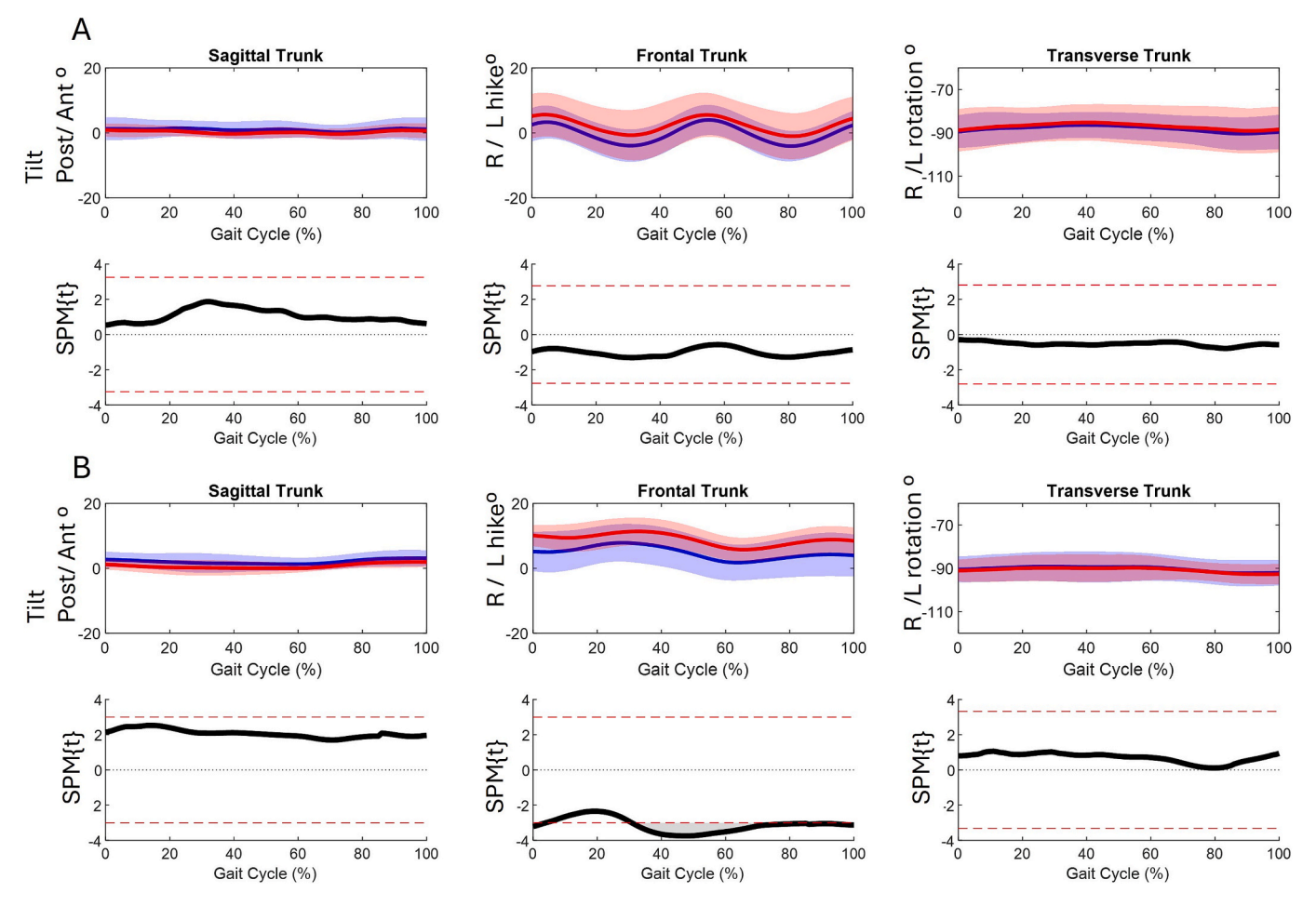


Fig. 2. Time-normalised mean (sold lines) trunk angles for the marker-based trials in blue and markerless trials in red for walking (A) and (B) trotting across 9 participants. The shaded areas indicate the \pm 1 SD between participants. SPM{t} results are plotted below each angle, illustrating significant differences (grey shaded regions) and the critical threshold (dashed red lines). (For interpretation of the references to colour in this figure legend, the reader is referred to the web version of this article.)

Helsinki principles for ethical research in human subjects. Human participants provided written informed consent, and the yard manager (responsible for horses' care) gave written informed consent for the horses included in the study.

2.2. Participants

Ten healthy female riders mean (SD) age: 34 (11) years, height: 169 (5) cm, mass: 64 (8) kg, volunteered for the study. Riders were required to have at least five years of riding experience and be approved as competent by the yard manager to participate in the study. Participants wore skin-tight clothing of contrasting colours, riding boots, and a helmet. Six healthy gelding horses from NTU Brackenhurst Equestrian Centre mean (SD) age: 16 (2) years, height: 162 (4) cm, mass: 577 (51) kg, were used. While the sample size was small, it was deemed appropriate for assessing the feasibility of the markerless system. Future research should include a larger, more diverse participant pool to strengthen the findings and enhance their generalisability. Horses were housed in individual stables, large multi-horse stables, or barn-style stables with access to small paddocks, based on individual needs. They are considered riding school horses, averaging 1-3 h of riding per day. Horses and riders were generally unfamiliar with each other. Data collection took place at NTU Brackenhurst Equestrian Centre from July 5th to 7th, 2022, between 9 am and 4 pm, in an indoor arena.

Experimental setup and procedure

A twelve-camera marker-based system (Qualisys Oqus 700, Qualisys

AB, Gothenburg, Sweden) and an eight-camera High Definition 2D video-based system (Qualisys Miqus, Qualisys AB, Gothenburg, Sweden) were used to collect data in a 55x40 metre indoor equestrian riding arena. Both systems were calibrated before data collection, with the largest accepted calibration error being 0.7 mm, representing the standard deviation in the known calibration wand length.

Motion capture data were collected synchronously at 85 Hz, 1080p. Marker cameras were placed on a tripod, and video cameras were attached via a clamp (Supplementary File 1). The marker-based cameras were situated to detect markers both on the rider's head and the horse's fetlock. Video cameras were positioned at a height approximately parallel to the rider's head, providing a predominantly planar view as recommended by Theia Markerless. This ensured participants were at least 500 pixels tall within the calibrated volume, maintaining the required 1080p resolution. The marker-based sampling rate was reduced to synchronise the data and ensure an adequate capture volume.

Forty-eight reflective markers (12 mm Ø) were fixed to each participant based on the IOR lower-limb and pelvis marker set (Leardini et al., 2007) and adapted plug-in-gait trunk and upper-limb marker set (Davis et al., 1991). The same investigator placed markers bilaterally on the pelvis and lower limbs at the following locations: medial malleoli, first, second and fifth metatarsal heads, posterior calcaneus, tibial tuberosity, fibula head, femoral epicondyles, greater trochanter, and anterior and posterior superior iliac spines. Trunk and upper limb markers were placed on the C7 and T10 vertebrae, jugular notch, xiphoid process, acromion processes, lateral and medial humeral

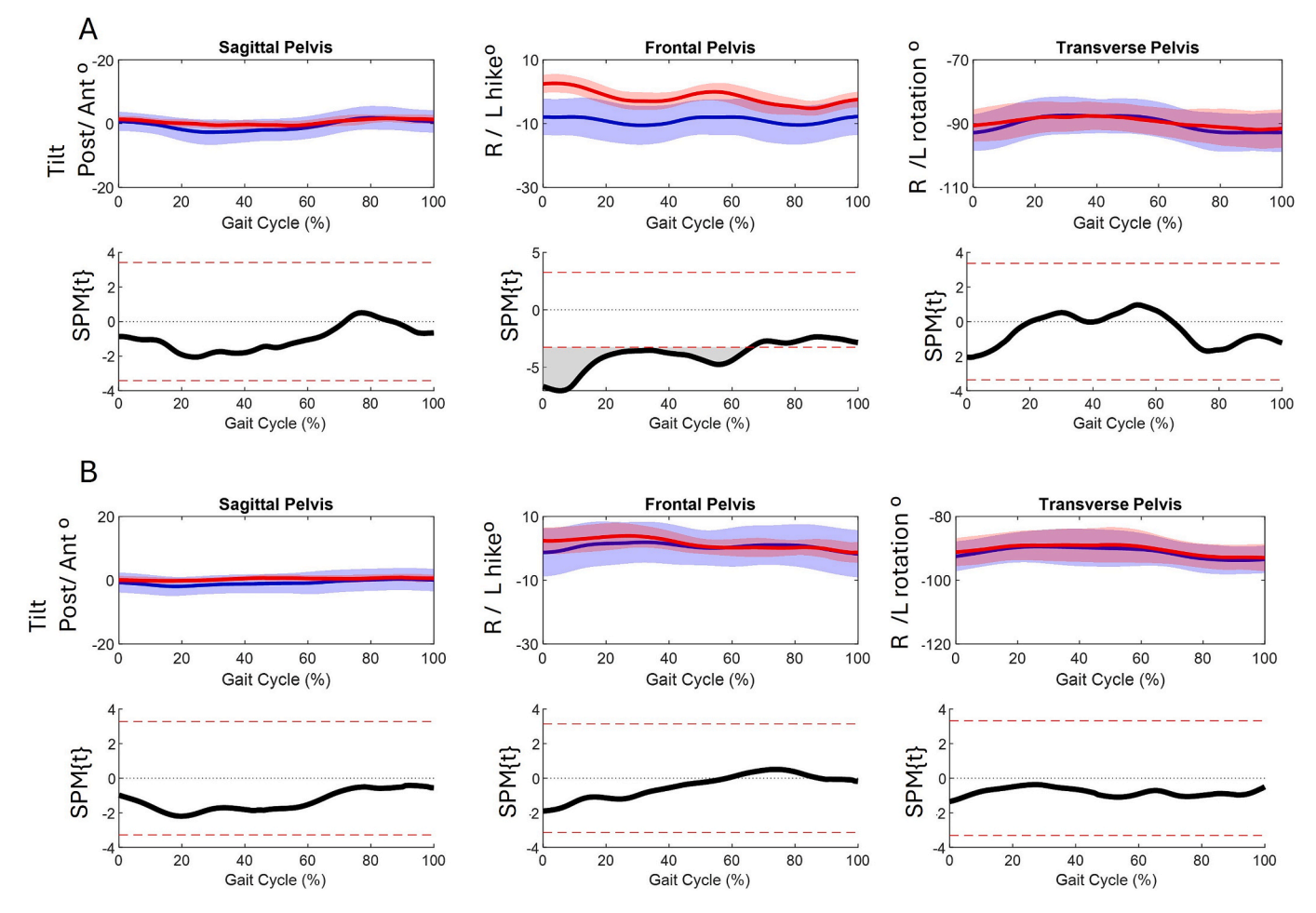


Fig. 3. Time-normalised mean (sold lines) pelvis angles for the marker-based trials in blue and markerless trials in red for walking (A) and (B) trotting across 9 participants. The shaded areas indicate the \pm 1 SD between participants. SPM{t} results are plotted below each angle, illustrating significant differences (grey shaded regions) and the critical threshold (dashed red lines). (For interpretation of the references to colour in this figure legend, the reader is referred to the web version of this article.)

epicondyles, styloid processes of the ulnar and radius, and head of the third metacarpal. Horses wore 30 mm diameter domed markers on the fetlock, attached to the lateral aspects of both hind and forelimbs to identify the gait cycle.

A static calibration trial for the marker-based motion capture was conducted with the participant standing on a mounting block to capture the correct height for riding. No static trial was required for the markerless system. The medial femoral and medial malleoli markers were removed before dynamic trials due to being obscured by the horse when the rider was mounted. Once mounted, riders completed a 10-minute walk and trot warm-up. Five dynamic trials at two self-selected speeds (walk and trot) were recorded for each horse and rider combination. The horse and rider moved through a channel, on the right rein, while cameras recorded the action (Fig. 1). All horses completed the activity, including the warm-up, within 60 min.

The retroreflective markers were digitised using Qualisys Track Manager (Qualisys, Gothenburg, Sweden) and exported for further analysis in Visual3D (HAS-Motion, Ontario, Canada). The global (lab) co-ordinate system was defined with the z-axis vertically, the y-axis along the rider's path (Fig. 1), and the x-axis towards the rider's right side. Joint centres were defined by the mid-point of corresponding medial and lateral anatomical markers for the wrist, elbow, knee, and ankle. The hip joint centre was defined by regression equations of pelvic markers (Bell et al., 1989), and the shoulder (glenohumeral joint centre) was located 5 cm distal to the right acromion (Kanko et al., 2021). The origin and local coordinate systems of each segment were defined by the

proximal joint centre. Visual3D computes the local axial (z) axis from the proximal and distal joint centres. The antero-posterior axis is defined by the plane of medial-lateral markers and the cross product of the z-axis vector. The medial-lateral axis is the cross product of the z and y axes. The trunk was defined from the midpoint between C7 and the jugular notch proximally, and between T10 and the xiphoid process distally. The axial (z) axis was the vector between the proximal and distal ends, the antero-posterior (y) axis was perpendicular to the plane of these markers, and the medial-lateral axis was the cross product of the z and y axes. The CODA pelvis model in Visual3D was used, with the origin at the midpoint of the anterior–superior iliac spine markers. The x-axis runs from the origin to the right ASIS, the z-axis is perpendicular to the (x-y) plane, and the y-axis is the cross product of the z and x axes.

The segments in the marker-based model were constrained to match those of the markerless system. A low-pass filter with a 6 Hz cut-off frequency was applied to the inverse kinematics model. Marker data were filtered with a bi-directional Butterworth filter with an 8 Hz cut-off frequency.

The markerless 2D video data were processed in Theia3D (v2021.2.0.1675) using a deep learning neural network for human feature recognition. The Theia lower-limb model was created with the pelvis having 6 degrees-of-freedom (DOF) and the hip and knee having 3 DOF. In the upper limb, the trunk had 6 DOF, the shoulder 3 DOF, and the elbow 2 DOF. The markerless data were filtered with a GCVSPL filter with an 8 Hz cut-off frequency. The markerless model is automatically defined in Visual3D using the pose from each 4x4 body segment matrix

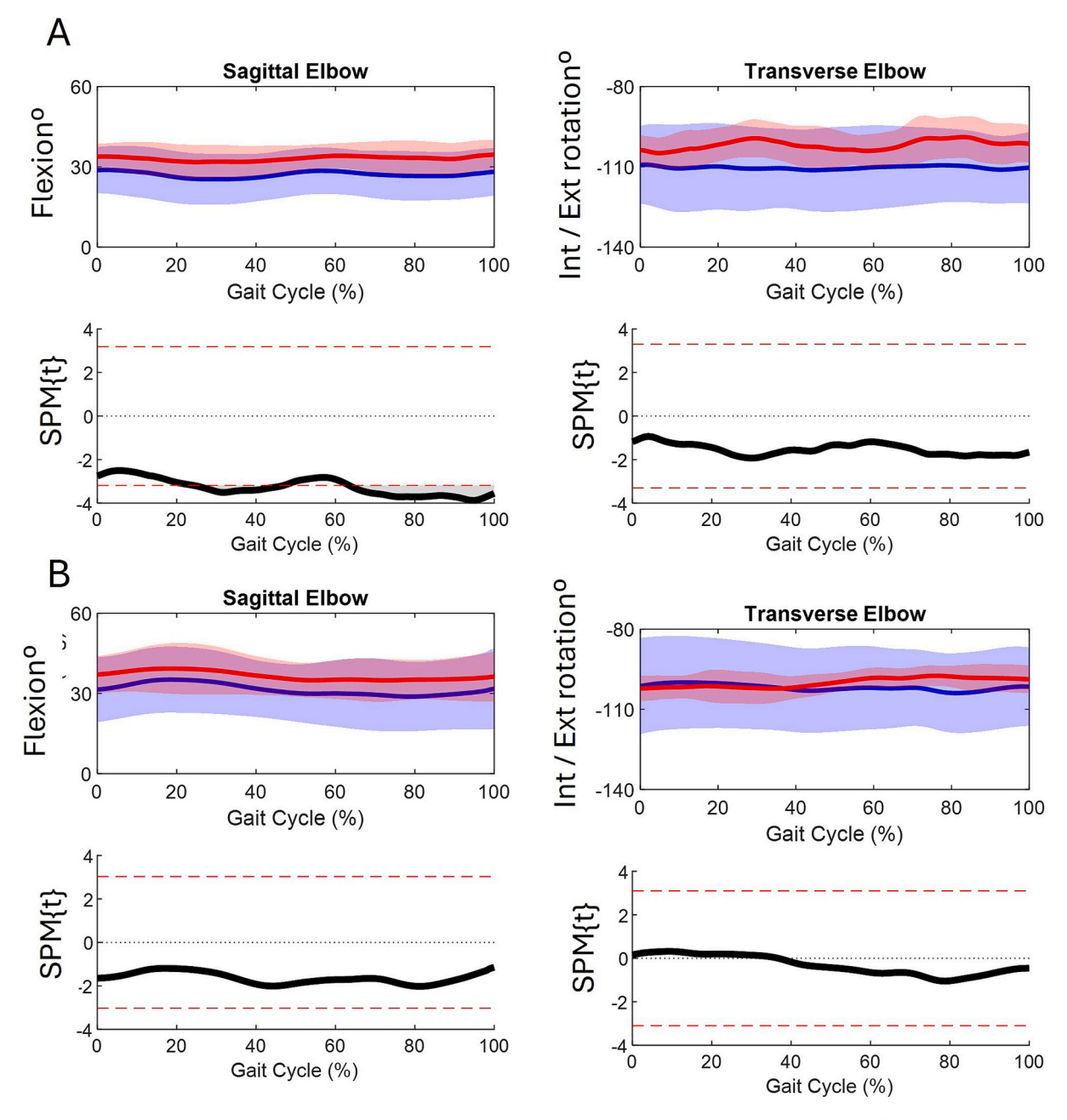


Fig. 4. Time-normalised mean (sold lines) left elbow angles for the marker-based trials in blue and markerless trials in red for walking (A) and (B) trotting across 9 participants. The shaded areas indicate the \pm 1 SD between participants. SPM{t} results are plotted below each angle, illustrating significant differences (grey shaded regions) and the critical threshold (dashed red lines). (For interpretation of the references to colour in this figure legend, the reader is referred to the web version of this article.)

from Theia. To compare the systems, 3D hip, knee, shoulder, and elbow joint angles were calculated using the Visual3D default X, Y, Z Carden sequence of rotations (Grood & Suntay, 1983). Additionally, trunk and pelvis segment angles relative to the global (lab) coordinate system were computed, with the Z-axis aligned vertically and the Y-axis anteriorly. Ankle data were excluded due to occlusion by the stirrups. For walk and trot, a gait cycle was defined from initial contact of the right hind-limb to the next initial contact of the right hind-limb. Gait cycles were identified by peaks in vertical acceleration of the marker on the right hind-limb fetlock, manually checked using video playback in Visual3D.

All joint and segment angles were time-normalised to 101 data points. The Root Mean Square Difference (RMSD) was calculated for each data point across the gait cycle and averaged across trials for each participant to quantify the mean offset between the systems. Results were summarised across participants to determine the mean and standard deviation (SD) RMSD. Statistical parametric mapping (SPM) paired t-tests were applied to the participant mean time-normalised curves (101 data points) in MatLab (R2023a, The Mathworks Inc., Natick, MA, USA). The source code was downloaded from https://spm1d.org/Downloads.html (accessed 20 January 2025). SPM reduces the chance of type 1 errors by overcoming the limitations of selecting random points in 1D data. Significance was indicated when SPM(t) values exceeded the critical threshold, calculated using random field theory on randomly smoothed data (Pataky et al., 2013), with an alpha level of 0.05.

3. Results

Joint angles are based on three to five trials per participant. Marker

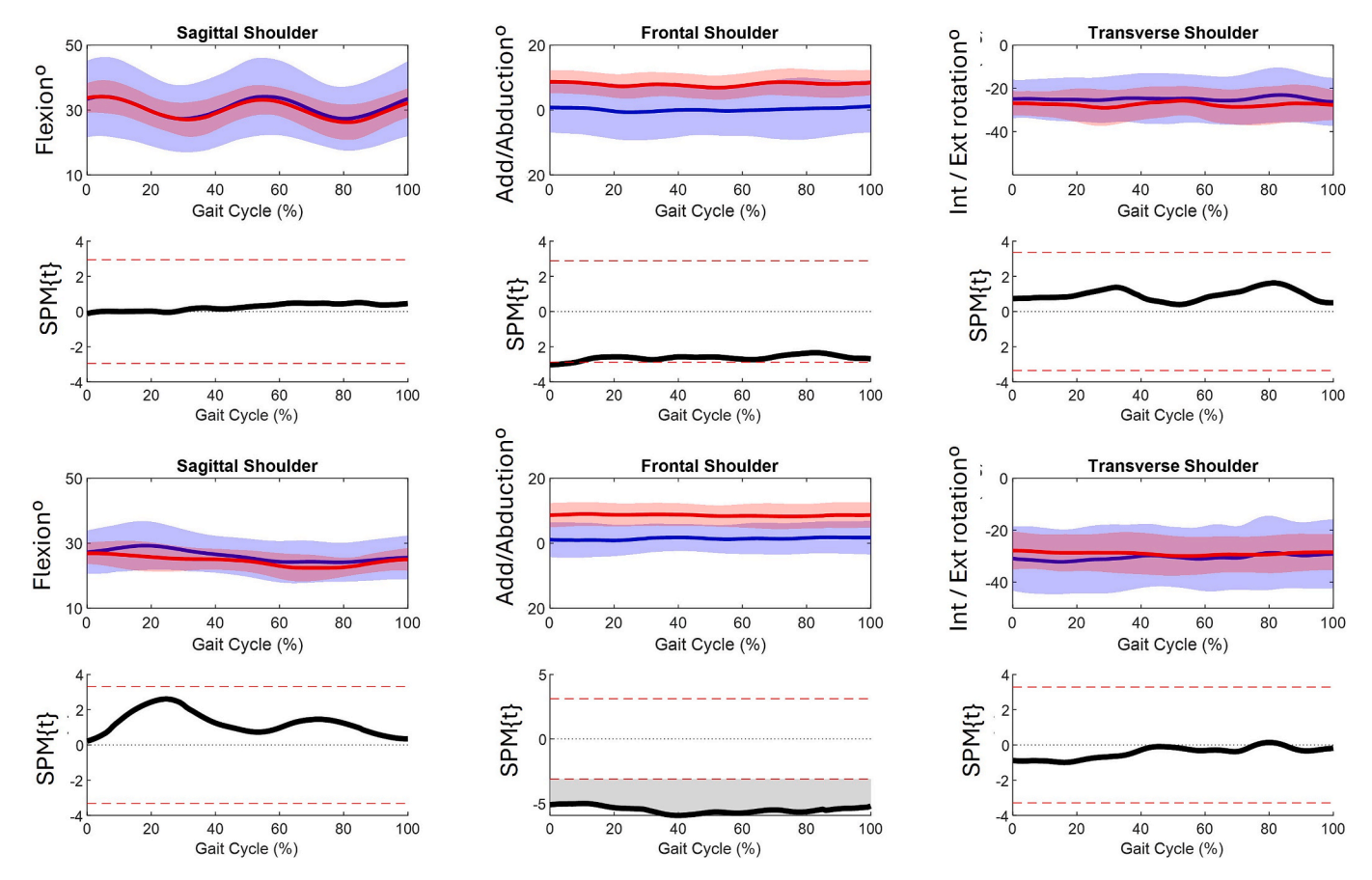


Fig. 5. Time-normalised mean (sold lines) left shoulder angles for the marker-based trials in blue and markerless trials in red for walking (A) and (B) trotting of 9 participants. The shaded areas indicate the \pm 1 SD between participants. SPM $\{t\}$ results are plotted below each angle, illustrating significant differences (grey shaded regions) and the critical threshold (dashed red lines). (For interpretation of the references to colour in this figure legend, the reader is referred to the web version of this article.)

occlusion or markers falling off prevented segment reconstruction for some participants. Results are based on 10 participants for the hip angle during walking and nine participants for all subsequent angles during walk and trot. Only trials with data from both systems were included. The RMSD in joint and segment angles between the marker-based and markerless systems are shown in Table 1. Mean segment/joint angles and SPM results are displayed for the trunk (Fig. 2), pelvis (Fig. 3), elbow (Fig. 4), shoulder (Fig. 5), hip (Fig. 6), and knee (Fig. 7).

For walking, the RMSD across sagittal, frontal, and transverse plane angles was 6.7° , 6.8° , and 9.3° , respectively. For trotting, the RMSD across these planes was 6.1° , 5.0° , and 9.3° , respectively. The difference between left and right limbs was less than 1° for 54 % of comparisons and less than 2° for 90 %. Therefore, we report SPM results for the left side only (Figs. 3-7). The RMSD range was 2.9° -19.1° for walking and 2.0° -18.8° for trotting. RMSD was typically higher in the transverse plane, with the smallest RMSD in the sagittal plane. An exception was that hip flexion RMSD was greater than external hip rotation values, particularly for walking.

SPM results showed no significant differences in the transverse plane for segment or joint angles. SPM paired t-tests revealed two significant sagittal plane differences during walking: increased hip flexion between 0–100 % (p < 0.001) (Fig. 6A) and elbow flexion between 24–47 % (p = 0.03) and 63–100 % (p < 0.001) of the gait cycle in the markerless system. Five significant results were found in the frontal plane. Pelvic drop increased in the marker-based system between 0–66 % (p < 0.001) of the walking gait cycle, with the left side higher (Fig. 3A). Trunk drop increased in the marker-based system between 31–65 % (p = 0.006) of the trotting gait cycle, with the left side higher (Fig. 2B). Shoulder adduction increased between 0–8 % (p = 0.049) during walking and

0--100 % (p <0.001) during trotting in the markerless system. Hip abduction increased in the markerless system between 0–11 % (p = 0.04), 17–26 % (p = 0.044), 41–43 % (p = 0.05), and 96–100 % (p = 0.05) during walking.

Pelvis and trunk segment angles had smaller RMSD values in the sagittal and transverse planes compared to upper and lower limb joint angles during walking and trotting.

4. Discussion

Markerless motion capture for riding opens up new research avenues in this field. The cost of markerless systems are reducing, set-up time is faster, post-processing is semi-automated, and there are no markers to interfere with natural movement or clothing. Data collection is therefore cheaper, more efficient, and requires less expertise. However, the accuracy of markerless motion capture for equestrian riders needs to be assessed. We compared joint and segment angles between marker-based and markerless systems of equestrian riders during walking and trotting, mounted on a horse.

Results showed that markerless system accuracy depended on the joint, plane, and gait. The RMSD offset was smaller in the sagittal plane, a trend also reported in people when walking (Kanko et al., 2021), running (Kanko et al., 2023), squatting, and forward hopping (Ito et al., 2022). In overground human locomotion, there is typically more joint range of motion in flexion/extension than in abduction/adduction or internal/external rotation, making frontal and transverse plane angles more prone to kinematic crosstalk from the sagittal plane (Piazza & Cavanagh, 2000). Therefore, it is not surprising that the difference between the two systems was larger outside the sagittal plane. However,

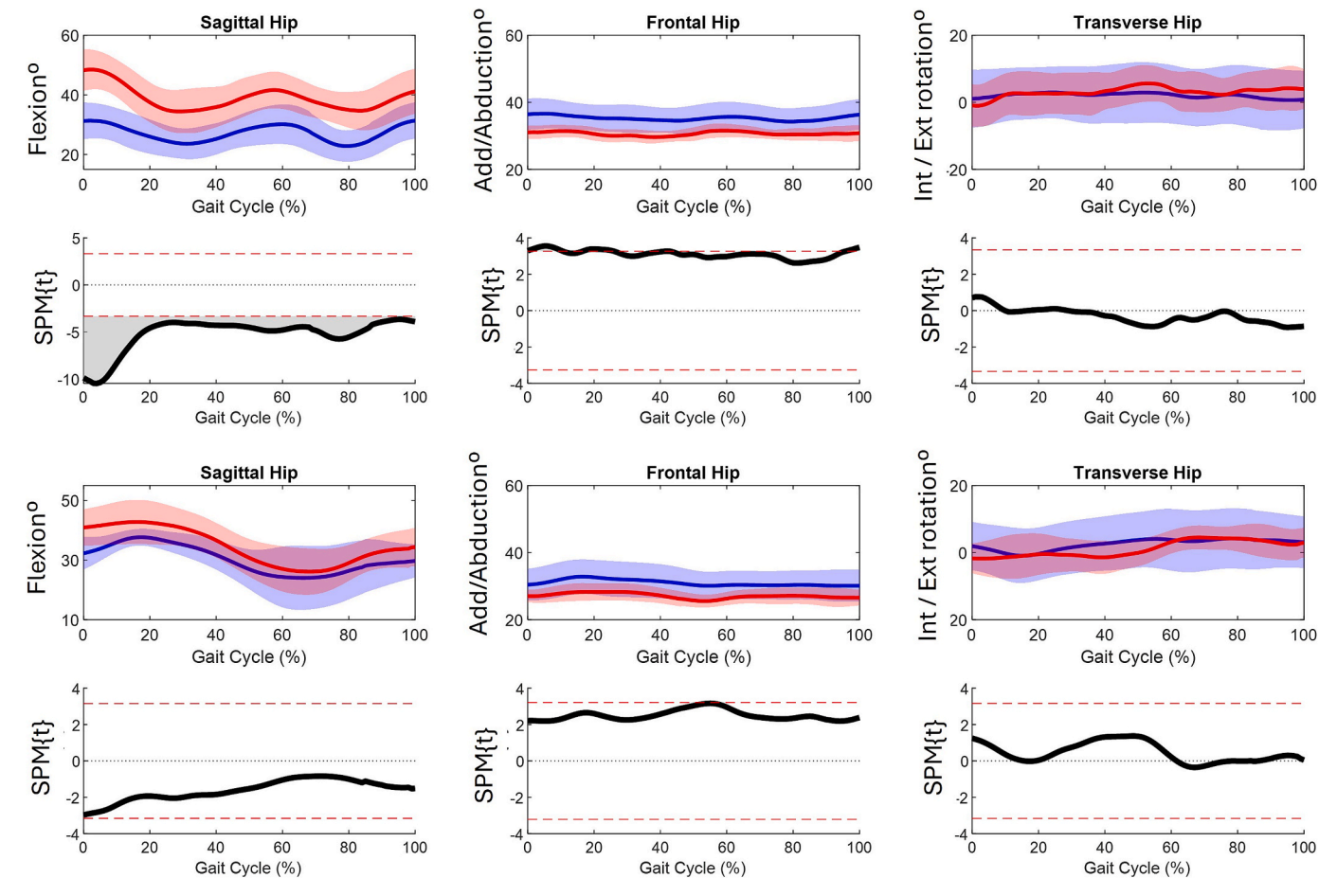


Fig. 6. Time-normalised mean (sold lines) left hip angles for the marker-based trials in blue and markerless trials in red for walking (A) and (B) trotting across 10 participants. The shaded areas indicate the \pm 1 SD between participants. SPM $\{t\}$ results are plotted below each angle, illustrating significant differences (grey shaded regions) and the critical threshold (dashed red lines). (For interpretation of the references to colour in this figure legend, the reader is referred to the web version of this article.)

most differences in frontal and transverse angles were under 10° , which may be acceptable dependent on the application. In our set-up, cameras were positioned along a channel (Fig. 1), perpendicular to the sagittal plane. In a static equestrian simulator, used in coaching, training, and research (Bye & Lewis, 2021; Wilkins et al., 2022), cameras could be positioned to improve accuracy along the frontal and transverse planes.

Markerless motion capture could be explored further within the context of equestrian simulators when used for therapeutic purposes, such as equine-assisted therapy, where precise movement analysis could improve rehabilitation strategies. Expanding research to include dynamic activities beyond walking and trotting, such as jumping or cantering, may provide additional insights into rider kinematics in higher-intensity scenarios. Future research could explore these applications to assess the feasibility of markerless systems across a broader range of equestrian activities.

SPM results showed systematic differences in the sagittal and frontal planes, suggesting the markerless system is not valid compared to the marker-based system. However, significant differences indicate more consistent RMSD across participants. Researchers should consider the effect of different models on segment POSE (Langley et al., 2021). While marker-based systems allow the user to define segment POSE, the Theia markerless model operates as a black box, which likely accounts for the observed sagittal and frontal plane offsets. No significant SPM results were found in the transverse plane, despite the largest RMSD values, suggesting transverse plane differences are unreliable. Some corrections could be considered for the frontal plane despite higher RMSD than the sagittal plane.

An exception to this trend was that hip flexion RMSD was greater than external rotation values, particularly during walking. Moreover, SPM found significantly increased hip and elbow flexion during walking, but not trotting. Riders remain seated during walking, whereas in trotting, they rise up and back down with each gait cycle (known as 'rising trot'). The rising trot likely improved accuracy in the markerless system due to greater hip range of motion and less obstruction of the medial leg by the horse.

The smallest RMSD differences were found for pelvis and trunk segment angles, with the pelvis differing by 4° and the trunk by 3° on average across both gaits and all planes. In fact, the sagittal and transverse plane both differed by less than 3° . These findings indicate that markerless motion capture is a suitable alternative for assessing trunk and pelvis motion in equestrian riders during walk and trot, being particularly accurate in the sagittal and transverse planes.

Human gait studies report increased error (RMSD: >6° by Wren et al., 2023 in clinical patients) and lower reliability (Carvalho et al., 2024) for pelvic tilt in healthy older adults compared to joint angles. This may be due to the different pelvis position during human gait, affecting segment angles. The increased similarity between systems for pelvis and trunk angles in this study could be because the entire segments were visible to cameras, unlike limbs, which were obscured by the horse or other body segments. Additionally, these segment angles were relative to the lab, not two segments relative to each other in the case of the joint angles. Thus, errors from multiple segments would result in larger total error. The trunk and pelvis segments are crucial in equestrian sports, as rider asymmetry can affect horse locomotion.

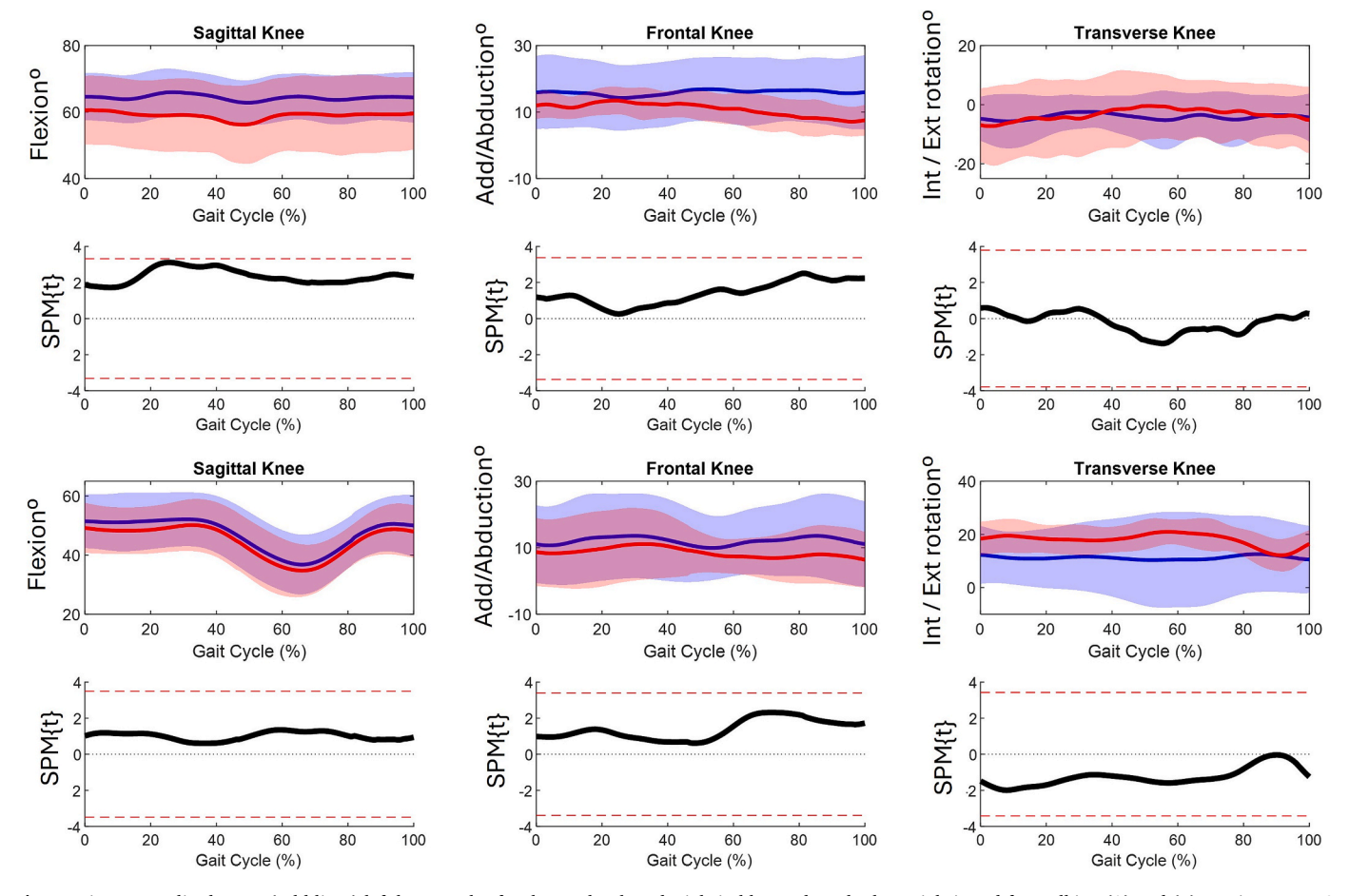


Fig. 7. Time-normalised mean (sold lines) left knee angles for the marker-based trials in blue and markerless trials in red for walking (A) and (B) trotting across 9 participants. The shaded areas indicate the \pm 1 SD between participants. SPM $\{t\}$ results are plotted below each angle, illustrating significant differences (grey shaded regions) and the critical threshold (dashed red lines). (For interpretation of the references to colour in this figure legend, the reader is referred to the web version of this article.)

MacKechnie-Guire et al. (2020) found that induced rider asymmetry significantly affected the kinematics of the thoracolumbar spine of horses. The standard protocol for assessing rider asymmetry involves 3D motion capture of the trunk and pelvis (Alexander et al., 2015), indicating that markerless motion capture could be useful for this area of equestrian kinematic analysis.

The largest segment angle differences were found in the transverse plane of the elbow. Equestrian riders maintain a slightly flexed elbow, parallel to the trunk, in a mostly static position (see Fig. 1 in Eckardt et al., 2014). This position causes the medial upper arm and elbow joint centre to be concealed by the trunk. This difference is likely unacceptably large for research or clinical applications. Future research using markerless technologies for rider training or biofeedback should focus on sagittal and frontal segment/joint angles with smaller RMSD until better accuracy is achieved in the transverse plane, especially at the elbow joint.

Ankle data was excluded due to occlusion by the stirrups, but this likely had little impact on the study findings, especially as transverse plane joint angles are the least comparable.

While marker placement variations can cause errors, markers in this study were placed by the same researcher. A systematic review of 3D kinematic gait measurements found that errors of 2° to 5° are reasonable but should be considered in data interpretation (McGinley et al., 2009). Leboeuf et al. (2019) also reported up to 3° error from joint center position estimations. Despite differences in camera numbers (12 for marker-based and 8 for markerless systems), this is unlikely to affect findings. A minimum of two cameras is required for marker tracking,

with three recommended to avoid occlusion. Therefore, more than the minimum number of cameras were used, and the markerless system is less susceptible to occlusions, using multiple perspectives and additional features for pose estimation. To minimise data gaps, four video cameras and six marker-based cameras were placed on each side of the channel (Fig. 1). While additional markerless cameras could improve accuracy, only a single horse gait cycle was needed. The systems were set up in an indoor arena with natural lighting, and camera settings were individually adjusted to maintain calibration and accuracy as per Theia recommendations. With the markerless software entire body positions are processed automatically which avoids markers being missed, data cannot be processed in real time due to the length of time taken post collection to analyse and apply the algorithm. So, if data processing fails or the video quality is poor, data were unusable.

This research is subject to limitations. As the first study to assess markerless technologies in horse riders, results suggest kinematics may be comparable to marker-based systems. However, the small sample size limits generalisability. Future studies can use this data for a priori power calculations to improve statistical power and allow broader conclusions on reliability and accuracy. Since this study, newer versions of the markerless software have been released, and updates may improve tracking accuracy, especially in the transverse plane. Future research should assess these advancements.

In conclusion, this is the first study to knowledge to identify that joint and segment angles from a markerless motion capture system were similar to a marker-based system on an equestrian rider. The trunk and pelvis segments were particularly comparable. Markerless systems could

be used in rider research and training biofeedback programs, given the observed errors relative to marker-based systems. They may be especially useful in simulated environments (e.g., riders mounted on equestrian simulators) for biofeedback and research. The joint angle results showed more variation, particularly in the transverse plane, meaning the accuracy of some angles may not be acceptable depending on the application.

Author Contributions.

Heather Cameron-Whytock: Conceptualisation; Data curation; Investigation; Methodology; Project administration; Resources; Writing – original draft; Writing – review & editing. Hannah Divall: Data curation; Formal analysis; Investigation; Methodology; Resources; Writing – original draft; Writing – review & editing. Martin Lewis: Formal analysis; Investigation; Methodology; Writing – review & editing. Charlotte Apps: Conceptualisation; Data curation; Formal analysis; Investigation; Methodology; Project administration; Resources; Writing – original draft; Writing – review & editing.

CRediT authorship contribution statement

Heather Cameron-Whytock: Writing – review & editing, Writing – original draft, Resources, Project administration, Methodology, Investigation, Data curation, Conceptualization. Hannah Divall: Writing – review & editing, Writing – original draft, Resources, Methodology, Investigation, Formal analysis, Data curation. Martin Lewis: Writing – review & editing, Methodology, Investigation, Formal analysis. Charlotte Apps: Writing – review & editing, Writing – original draft, Resources, Project administration, Methodology, Investigation, Formal analysis, Data curation, Conceptualization.

Declaration of competing interest

Martin Lewis works for the company that sells the hardware and software used in this study (Qualisys). No other competing interests to declare.

The authors declare that they have no known competing financial interests or personal relationships that could have appeared to influence the work reported in this paper.

Acknowledgements

The authors would like to acknowledge Jodie Levick for helping with data collection.

Appendix A. Supplementary data

Supplementary data to this article can be found online at https://doi.org/10.1016/j.jbiomech.2025.112728.

References

- Alexander, J., Hobbs, S.J., May, K., Northrop, A., Brigden, C., Selfe, J., 2015. Postural characteristics of female dressage riders using 3D motion analysis and the effects of an athletic taping technique: a randomised control trial. Phys. Ther. Sport 16 (2), 154-161.
- Bennet, E.D., Cameron-Whytock, H., Parkin, T.D., 2023a. Fédération Equestre Internationale eventing: Fence-level risk factors for falls during the cross-country phase (2008–2018). Equine Vet. J. 55 (3), 463–473.
- Bennet, E.D., Parkin, T., Cameron-Whytock, H., 2023b. We have demonstrated the potential to make eventing safer: What will happen next? Equine Vet. J.
- Bennet, E.D., Cameron-Whytock, H., Parkin, T.D., 2022. Fédération Equestre Internationale eventing: Risk factors for horse falls and unseated riders during the cross-country phase (2008-2018). Equine Vet. J. 54 (5), 885–894.
- Bye, T.L., Lewis, V., 2021. Footedness and Postural Asymmetry in Amateur Dressage Riders, Riding in Medium Trot on a Dressage Simulator. J. Equine Vet. 102, 103618.
- Byström, A., Roepstroff, L., Geser-von Peinen, K., Weishaupt, M.A., Rhodin, M., 2015. Differences in rider movement pattern between different degrees of collection at the trot in high-level dressage horses ridden on a treadmill. Hum. Mov. Sci. 41, 1–8.

- Cameron-Whytock, H.A., Parkin, T.D., Hobbs, S.J., Brigden, C.V., Bennet, E.D., 2024. Towards a safer sport: Risk factors for cross-country horse falls at British Eventing competition. Equine Vet. J. 56 (1), 137–146.
- Carvalho, A., Vanrenterghem, J., Cabral, S., Assunção, A., Fernandes, R., Veloso, A.P., Moniz-Pereira, V., 2024. Markerless three-dimensional gait analysis in healthy older adults: test-retest reliability and measurement error. J. Biomech. 174, 112280.
- Clark, L., Bradley, E.J., Mackechnie-Guire, R., Taylor, A., Ling, J., 2022. Trunk kinematics of experienced riders and novice riders during rising trot on a riding simulator. J. Equipe Vet. 119, 104163.
- Davis III, R., Ounpuu, S., Tyburski, D., Gage, J., 1991. A gait analysis data collection and reduction technique. Hum. Mov. Sci. 10, 575–587.
- Foreman, M.H., Engsberg, J.R., Foreman, J.H., 2019. Point mass impulse-momentum model of the equine rotational fall. Comp. Exercise Physiol. 15 (3), 157–166.
- Eckardt, F., Münz, A., Witte, K., 2014. Application of a full body inertial measurement system in dressage riding. J. Equine Vet. 34 (11–12), 1294–1299.
- Engell, M.T., Clayton, H.M., Egenvall, A., Weishaupt, M.A., Roepstorff, L., 2016. Postural changes and their effects in elite riders when actively influencing the horse versus sitting passively at trot. Comp. Exercise Physiol. 12 (1), 27–33.
- Gandy, E.A., Bondi, A., Hogg, R., Pigott, T.M., 2014. A preliminary investigation of the use of inertial sensing technology for the measurement of hip rotation asymmetry in horse riders. Sports Technology 7 (1–2), 79–88.
- Grood, E. S., & Suntay, W. J. (1983). A joint coordinate system for the clinical description of three-dimensional motions: application to the knee.
- Ito, N., Sigurŏsson, H.B., Seymore, K.D., Arhos, E.K., Buchanan, T.S., Snyder-Mackler, L., Silbernagel, K.G., 2022. Markerless motion capture: What clinician-scientists need to know right now. JSAMS plus 1, 100001.
- Kanko, R.M., Laende, E.K., Davis, E.M., Selbie, W.S., Deluzio, K.J., 2021. Concurrent assessment of gait kinematics using marker-based and markerless motion capture. J. Biomech. 127, 110665.
- Kanko, R.M., Outerleys, J.B., Laende, E.K., Scott Selbie, W., Deluzio, K.J., 2023. Comparison of concurrent and asynchronous running kinematics and kinetics from marker-based motion capture and markerless motion capture under two clothing conditions. BioRxiv 2023.
- Langley, B., Jones, A., Board, T., Greig, M., 2021. Modified conventional gait model vs.
 Six degrees of freedom model: A comparison of lower limb kinematics and associated error. Gait Posture 89, 1–6.
- Leardini, A., Sawacha, Z., Paolini, G., Ingrosso, S., Nativo, R., Benedetti, M.G., 2007. A new anatomically based protocol for gait analysis in children. Gait Posture 26 (4), 560–571.
- Leboeuf, F., Baker, R., Barré, A., Reay, J., Jones, R., Sangeux, M., 2019. The conventional gait model, an open-source implementation that reproduces the past but prepares for the future. Gait Posture 69, 235–241.
- MacKechnie-Guire, R., MacKechnie-Guire, E., Fairfax, V., Fisher, M., Hargreaves, S., Pfau, T., 2020. The effect that induced rider asymmetry has on equine locomotion and the range of motion of the thoracolumbar spine when ridden in rising trot. J. Equine Vet. 88, 102946.
- McGinley, J.L., Baker, R., Wolfe, R., Morris, M.E., 2009. The reliability of threedimensional kinematic gait measurements: a systematic review. Gait Posture 29 (3), 360–369.
- Pataky, T.C.; Robinson, M.A.; Vanrenterghem, J. 2013. Vector field statistical analysis of kinematic and force trajectories. J. Biomech. 3, 46, 2394–2401.
- Piazza, S.J., Cavanagh, P.R., 2000. Measurement of the screw-home motion of the knee is sensitive to errors in axis alignment. J. Biomech. 33 (8), 1029–1034.
- Rhodin, M., Byström, A., Roepstorff, L., Hernlund, E., Van Weeren, P.R., Weishaupt, M. A., Egenvall, A., 2018. Effect of different head and neck positions on kinematics of elite dressage horses ridden at walk on treadmill. Comp. Exercise Physiol. 14 (2), 69–78.
- Robert-Lachaine, X., Mecheri, H., Larue, C., Plamondon, A., 2017. Validation of inertial measurement units with an optoelectronic system for whole-body motion analysis. Med. Biol. Eng. Compu. 55, 609–619.
- Song, K., Hullfish, T.J., Silva, R.S., Silbernagel, K.G., Baxter, J.R., 2023. Markerless motion capture estimates of lower extremity kinematics and kinetics are comparable to marker-based across 8 movements. J. Biomech. 157, 111751.
- Stanev, D., Filip, K., Bitzas, D., Zouras, S., Giarmatzis, G., Tsaopoulos, D., Moustakas, K., 2021. Real-time musculoskeletal kinematics and dynamics analysis using markerand IMU-based solutions in rehabilitation. Sensors 21 (5), 1804.
- Strutzenberger, G., Kanko, R., Selbie, S., Schwameder, H., Deluzio, K., 2021. Assessment of kinematic CMJ data using a deep learning algorithm-based markerless motion capture system. ISBS Proceedings Archive 39 (1), 236.
- Walker, A.M., Applegate, C., Pfau, T., Sparkes, E.L., Wilson, A.M., Witte, T.H., 2016. The kinematics and kinetics of riding a racehorse: A quantitative comparison of a training simulator and real horses. J. Biomech. 49 (14), 3368–3374.
- Wilkins, C.A., Wheat, J.S., Protheroe, L., Nankervis, K., Draper, S.B., 2022. Coordination variability reveals the features of the 'independent seat'in competitive dressage riders. Sports Biomech. 1–16.
- Wren, T.A., Isakov, P., Rethlefsen, S.A., 2023. Comparison of kinematics between Theia markerless and conventional marker-based gait analysis in clinical patients. Gait Posture 104, 9–14.
- Zhang, J.T., Novak, A.C., Brouwer, B., Li, Q., 2013. Concurrent validation of Xsens MVN measurement of lower limb joint angular kinematics. Physiol. Meas. 34 (8), N63.